

## CONDENSATION INDUCED WATER HAMMER IN STEAM GENERATORS\*

by

O.C. Jones, Jr., P. Saha, B.J.C. Wu, and T. Ginsberg

Nuclear Safety Programs - Department of Nuclear Energy  
Brookhaven National Laboratory, Upton, New York 11973

June 1979

MAILED

## ABSTRACT

The case of condensation induced water hammer in nuclear steam generators is summarized, including both feed ring-type and economizer-type geometries. A slug impact model is described and used to demonstrate the parametric dependence of the impact pressures on heat transfer rates, initial pressures, and relative initial slug and void lengths. The results of the parametric study are related also to the economizer geometry and a suggested alternative model is presented. The importance of concerns regarding attenuation of shocks in two-phase media is delineated, and a simple experiment is described which was used to determine negligible attenuation within the accuracy of the experiment for void fractions up to over 30% in bubbly and slug flows.

Manuscript Prepared for Presentation at the Joint  
U.S. - Japan Information Exchange on Two-Phase Flow Dynamics  
Osaka University, Osaka, Japan  
August 1-3, 1979

\*Work performed under the auspices of the U.S. Nuclear Regulatory Commission

## DISCLAIMER

This book was prepared as an account of work sponsored by, or on behalf of, the United States Government. Neither the United States Government nor any agency thereof, nor any of their employees, makes any warranty, express or implied, or assumes any legal liability or responsibility for the accuracy, completeness, or usefulness of any information, apparatus, product, or process disclosed, or represents that its use would not infringe privately owned rights. Reference herein to any specific commercial product, process, or service by trade name, trademark, manufacturer, or otherwise, does not necessarily constitute or imply its endorsement, recommendation, or favoring by the United States Government or any agency thereof. The views and opinions of authors expressed herein do not necessarily state or reflect those of the United States Government or any agency thereof.

DISTRIBUTION OF THIS DOCUMENT IS UNLIMITED

TABLE OF CONTENTS

LIST OF FIGURES . . . . .	iii
LIST OF TABLES. . . . .	iii
NOMENCLATURE. . . . .	iv
1. INTRODUCTION. . . . .	1
2. BACKGROUND. . . . .	1
3. SLUG IMPACT MODEL ANALYSIS. . . . .	3
4. CALCULATED RESULTS. . . . .	6
5. INTERNAL VOID COLLAPSE CONSIDERATIONS . . . . .	10
6. PRESSURE PULSE ATTENUATION EXPERIMENTS. . . . .	12
7. CONCLUSIONS AND RECOMMENDATIONS . . . . .	14
8. ACKNOWLEDGEMENTS. . . . .	15
9. REFERENCES. . . . .	15

## LIST OF FIGURES

<u>Figure</u>		<u>Page</u>
1	Model for slug impact water hammer analysis	3
2	Effect of heat transfer coefficient on cavity length	8
3	Effect of heat transfer coefficient on cavity pressure	8
4	Effect of heat transfer coefficient on slug velocity	8
5	Effect of heat transfer coefficient on slug impact pressure	8
6	Effect of initial pressure on cavity length	10
7	Effect of initial pressure in cavity pressure	10
8	Effect of initial pressure on slug impact pressure	10
9	Effect of initial relative cavity length on instantaneous cavity size	11
10	Effect of initial relative cavity length on cavity pressure	11
11	Effect of initial relative cavity length on impact pressure	11
12	Effect of geometric scale. Solid line - 1/8-scale, $t^*=t$ . Dashed line - full scale, $t^*=t/8$ . $p_0=20$ bar	11
13	Schematic diagram of the shock tube experimental rig	12
14	Shock tube results for transducers 12, 13, and 14, for 100% air	13
15	Shock tube results for transducers 12, 13, and 14, for 100% water	13
16	Shock tube results typical of two-phase bubbly flow	14
17	Shock tube results typical of two-phase slug flow	14

## LIST OF TABLES

TABLE 1	Conditions chosen for parametric evaluation of the slug impact model. Pipe diameter, 4.3 cm; Feedwater velocity, 0.9125 m/s; Water temperature, 27C.	7
---------	--	---

## NOMENCLATURE

### English

A Cross sectional pipe area  
a Sonic velocity  
c Mass concentration  
D Diameter  
 $\bar{f}$  Friction coefficient  
G Mass flux  
h Heat transfer coefficient  
i specific enthalpy  
p pressure  
Q Total heat input rate  
 $q''$  heat flux  
T Temperature  
t time  
v velocity  
z axial location

### Greek

$\Gamma$  Volumetric vapor generation rate  
 $\rho$  Fluid density  
 $\xi$  Heated perimeter

### Subscripts

o Interface "o"  
1 Interface "1"  
2 Interface "2"  
 $fg$  Liquid-to-vapor difference  
 $fw$  Feed water  
i Interface or impace  
in Into the section considered  
l Liquid  
m mixture  
out Out of section considered  
s Saturation  
v Vapor  
\* Modified as denoted

## INTRODUCTION

In the eventuality of a loss of off-site power, (estimated to occur once every 1 to 1 1/2 plant years), the liquid level in the secondary side of a feeding type steam generator may drop below the feedwater inlet before auxiliary power becomes available and cold auxiliary water begins to be fed into the system. If the feedwater line is horizontal and has drained sufficiently during the time power was unavailable, a severe water hammer event may occur. Indeed, such events have been recorded such as at the Tihange site. In fact, significant damage to the main feedwater pipe of Indian Point #2 plant occurred November 13, 1973<sup>[1]</sup> when cold auxiliary water was introduced into the steam generator. It is believed that the damage was due to a severe impact of water slug in the feedwater piping system. This and several other less damaging incidents of water hammer in steam generators recently became of concern to the nuclear industry.

A firm understanding of the potential for condensation-induced water hammer in PWR steam generators does not currently exist. For top-feed systems, a potential model has been proposed<sup>[2]</sup> where liquid slug formation occurs due to condensation-induced counterflow in horizontal lines followed by slug acceleration and impact in the blind end of the horizontal run. Visual observation lends support to this slug impact model. Quantitative confirmation, however, has not been established under any circumstances including prototypical conditions. Certain combinations of "ad hoc" fixes (i.e., J-tubes and short horizontal runs), seem to work at low pressure in small geometries. These fixes have been recommended and in some cases implemented in several operating plants. An understanding as to why they work, if in fact they do, is currently lacking.

At this time a potential model for water hammer due to bottom (economizer) emergency cold feedwater injection in either Westinghouse or Combustion Engineering steam generators does not exist. Westinghouse has conducted small scale tests,<sup>[3]</sup> but these have not served to resolve this question. Virtually no knowledge, analysis, or testing regarding the potential for localized void collapse and pressure pulse formation in interior regions of steam generators exists. A significant part of the question of potential tube rupture in such cases rests on knowledge of shock attenuation in two-phase mixtures or through tube bundles which appears to be lacking.

Scaling laws do not presently exist enabling small scale experimental results on condensation-induced water hammer obtained either at off-plant conditions or at actual operating pressures to be extrapolated to full scale actual conditions. It is unclear in view of the current lack of knowledge whether a real safety problem may exist.

It is the purpose of this paper to present the results of a parametric model for slug impact-induced water hammer and to describe an experiment designed to provide direction regarding the potential for two-phase mixture to mitigate the effects of localized void collapse induced pressure pulses through attenuation of the resulting shock waves.

## BACKGROUND

Current nuclear steam generators generally fall into three classes: upper injection types utilizing a single feedwater inlet and internal feeding distributor; lower injection or "economizer" types having a single feedwater inlet into either an annular downcomer or toward a vertical diffuser plate;

upper injection types having multiple pressure vessel inlet ports with upward-slanting inlet piping tied to an external header, (used in Babcock and Wilcox steam generators). In the last type the feed lines can not drain due to low level in the steam generator since the inlet pipes slope downward away from the pressure vessel. The first type comprises the majority of those currently in service while the economizer designs are relatively new with no plants yet in service. (The first economizer type will be the McGuire plant being constructed for Duke Power.) As mentioned in the introduction, it is the feeding design which has experienced difficulties.

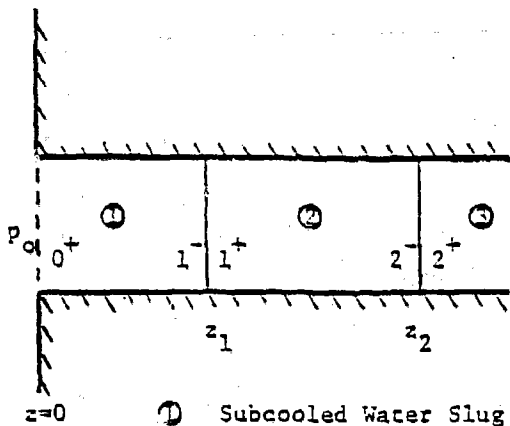
Several "ad hoc" fixes were proposed to circumvent the problem without really understanding the basic mechanism of the water hammer. In fact, modifications were proposed by Westinghouse to utilities having this type of steam generator. These modifications, although quite costly, were to reduce the chance that such an event might occur.

In response to the increased awareness of the potential for severe water hammer, NRC sponsored a study by Creare, Inc.<sup>[2]</sup> to try to rationalize the sequence of events that could lead to the severe impact on the piping system. It was determined experimentally in the Creare Study that, while the addition of J-tubes, (top discharge), to the feeding, or the decrease in feedwater line length had only small effects by themselves, the combination of the two had a major effect in reducing or eliminating condensation-induced water hammer. It was postulated that if the feeding is allowed to drain prior to cold auxiliary feedwater injection, water slugs might be formed which would trap steam voids, and rapid condensation of these trapped voids by incoming cold water would cause the water slugs to accelerate and impact on the blind end of the feedwater piping system.

Based on small-scale tests, Creare, Inc. recommended a combination of fixes, e.g., top discharge with J-tubes, short horizontal length of the feedpipe, an upper limit of auxiliary feedwater flow rate, etc., to avoid the possibility of having severe water hammers. All new plants with feeding type steam generators are now required to abide by NRC rules in line with Creare recommendation, and undergo confirmatory testing. However, some older plants do not have the combination recommended by Creare, and thus may be more susceptible to damaging water hammer than others. From the preceding remarks it appears obvious that for the top feed type steam generators, there is no clear foundation of technical understanding upon which to make licensing decisions regarding plant safety. This appears true in spite of the fact that several "ad hoc" methods based on qualitative, low pressure, small scale tests have been proposed, and in some cases implemented, with the idea of decreasing the probability of water hammer occurring.

In an apparent attempt to eliminate the possibility of top auxiliary feedwater leading to a severe water hammer event, as well as to solve some other existing difficulties, both Westinghouse and Combustion Engineering introduced new, economizer, designs. In these new designs the feedwater will be introduced low in the secondary side being directed either into a diffuser plate or a vertical, annular downcomer.

NRC was concerned with introduction of the new preheater-type steam generator design. Perhaps a damaging water hammer could occur at or near the preheater section. In an attempt to answer these concerns, Westinghouse conducted a 1/8-th-scale test program<sup>[3]</sup> to study the possibility of condensation-induced water hammer in the preheater section. They also proposed scaling criteria to extrapolate their 1/8-scale test results to full-scale steam generators. Brookhaven National Laboratory (BNL) was requested by NRC to



- ① Subcooled Water Slug  
 ② Vapor Cavity  
 ③ Subcooled Feed Water

Figure 1. Model for slug impact water hammer analysis. (No BNL Neg.)

evaluate these test results and scaling laws. Although some questions regarding the adequacy of the Westinghouse tests are yet to be resolved, it was, however, concluded by BNL [4] that a meaningful scaling criterion cannot be derived at this point because of the uncertainties in the condensation rate and the ratio between the initial water slug volume and the vapor cavity volume. On the other hand, it appeared that for one of the designs, an engineered approach reduced the probability of cold water being injected into the economizer section.

In what follows, attention will be drawn to the feeding-type steam generator and an analysis will indicate the parametric effects of condensation rates, pressure, slug lengths, and pipe size.

#### SLUG IMPACT MODEL ANALYSIS

The geometry of concern is shown in Figure 1 where it is assumed that a cylindrical water slug of length ND has been formed at rest in a pipe of diameter D. Initial water temperature is generally taken to be at room temperature and the instantaneous steam temperature is taken as the equilibrium saturation value for the given pressure. Condensation is assumed to occur at the steam-water interfaces located at  $z_1$  and  $z_2$  only. Compressibility of the liquid is ignored.

#### Water Slug

The conservation equations of mass, momentum, and energy are

$$\text{mass: } \frac{\partial \rho_2}{\partial t} + \frac{\partial G}{\partial z} = 0 \quad (1)$$

$$\text{momentum: } \frac{\partial G}{\partial t} + \frac{\partial}{\partial z} \left( \frac{G^2}{\rho_2} \right) = \frac{\partial p}{\partial z} - \frac{f|G|G}{2D\rho_2} \quad (2)$$

$$\text{energy: } \frac{\partial i_2}{\partial t} + \frac{G}{\rho_2} \frac{\partial i_2}{\partial z} = - \frac{1}{\rho_2} \frac{dq''}{dz} - \frac{\partial p}{\partial t} \quad (3)$$

It has been assumed that the wall is adiabatic so only the axial heat flux term has been retained in (3). The constant liquid density assumption allows

Equation (1) to be integrated to give

$$\langle G \rangle_1 = G_{0+} = G_{1-} \quad (4)$$

where the  $\langle \rangle$  symbols represent volume averaged quantities.

Integration of the momentum equation spatially, including application of Leibnitz rule results in

$$\frac{d\langle G \rangle_1}{dt} = - \frac{\langle p_2 \rangle - p_0}{z_1} - \frac{\bar{f} \langle G \rangle_1}{2D \langle \rho_2 \rangle_1} \quad (5)$$

Similarly, the energy equation is integrated with the assumption of uniform temperature in the liquid, ( $i_{1-} = \langle i \rangle_1$ ), so that

$$\frac{d\langle i \rangle_1}{dt} = \frac{\langle G \rangle_1}{\rho_2 z_1} (i_{0+} - \langle i \rangle_1) - \frac{\dot{q}_1''}{\rho_2 z_1} \quad (6)$$

where the heat flux is given as

$$\dot{q}_1'' = h_{21} [\langle T \rangle_1 - T_s \langle \rho \rangle_2] \quad (7)$$

Equations of state are used to denote the density and temperature of the liquid slug in terms of the liquid enthalpy and the average slug pressure.

### Vapor Cavity

Conservation equations for the vapor cavity include

$$\text{mass:} \quad \frac{\partial \rho}{\partial t} + \frac{\partial G}{\partial z} = 0 \quad (8)$$

$$\text{momentum:} \quad \langle p \rangle_2 = f(t) \quad (9)$$

$$\text{energy:} \quad \frac{\partial(\rho i - p)}{\partial t} + \frac{\partial(iG)}{\partial z} = - \frac{\partial \dot{q}_1''}{\partial z} + \frac{\dot{q}_w'' \xi_w}{A} \quad (10)$$

where friction and inertia are ignored, and an equation of state (caloric) will be used to determine  $f(t)$  for the instantaneous cavity pressure.



Integration of (8) for the vapor cavity yields

$$(Z_2 - Z_1) \frac{d\langle \rho_m \rangle_2}{dt} + G_{2-} - G_{1+} = 0 \quad (11)$$

while the energy equation integrated over the steam cavity volume using Leibnitz rule results in

$$\begin{aligned} & (Z_2 - Z_1) \frac{d}{dt} \left[ \langle \rho_m \rangle_2 \langle i_m \rangle_2 - \langle p \rangle_2 \right] + (G_{2-} i_m) |_{2-} - (G_{1+} i_m) |_{1+} \\ & = \dot{q}_{1+}'' - \dot{q}_{2-}'' + \frac{\langle \dot{q}_w'' \rangle (Z_2 - Z_1) \xi_w}{A} \end{aligned} \quad (12)$$

Now the assumption of uniform temperature and pressure in the vapor cavity results in  $i_{m2-} = i_{m1+} = \langle i_m \rangle_2$ . Also, the net heat flux out of the vapor cavity is expressed as

$$\sum \dot{q}_{out}'' \equiv \dot{q}_{2-}'' - \dot{q}_{1+}'' = (h_{v2} + h_{v1}) \left[ \langle T \rangle_2 - T_s \langle p \rangle_2 \right] \quad (13)$$

The equation of state for the mixture density in terms of enthalpy and pressure yields

$$\frac{d\langle \rho_m \rangle_2}{dt} = \left( \frac{\partial \rho_m}{\partial i_m} \right) \langle p \rangle_2 \frac{d\langle i_m \rangle_2}{dt} + \left( \frac{\partial \rho_m}{\partial p} \right) \langle i_m \rangle_2 \frac{d\langle p \rangle_2}{dt} \quad (14)$$

Linear combination of Equations (11), (12), and (14) gives two coupled ordinary differential equations in terms of pressure and enthalpy given by

$$(Z_2 - Z_1) \frac{d\langle p \rangle_2}{dt} = \frac{(G_{2-} - G_{1+}) \langle p \rangle_2 \left( \frac{\partial i_m}{\partial p} \right)_{\langle \rho_m \rangle_2} - \sum \dot{q}_{out}'' + \dot{Q}_{in,w}/A}{\left[ \langle \rho_m \rangle_2 \left( \frac{\partial i_m}{\partial p} \right)_{\langle \rho_m \rangle_2} - 1 \right]} \quad (15)$$

and

$$(Z_2 - Z_1) \frac{d\langle h_m \rangle_2}{dt} = \frac{(Z_2 - Z_1)}{\langle \rho_m \rangle_2} \frac{d\langle p \rangle_2}{dt} - \frac{1}{\langle \rho_m \rangle_2} \left[ \sum \dot{q}_{out}'' - \dot{Q}_{in,w} A \right] \quad (16)$$

## Interface Equations

For compatibility between the water slug and the vapor cavity, the appropriate interface jump balance Equations are used including

$$\text{mixture mass jump: } (G - \rho_m \dot{Z}_1)_{1^-} = (G - \rho_m \dot{Z}_1)_{1^+} \quad (17)$$

$$\text{vapor mass jump: } [c(G - \rho_m \dot{Z}_1)]_{1^+} = [c(G - \rho_m \dot{Z}_1)]_{1^-} + \Gamma_{i1} \quad (18)$$

Now  $c_{1^-} = 0$ , and  $c_{1^+} = \langle c \rangle_2$ , while  $z_1 = z_{1^-}$  so that these two relations yield

$$\dot{Z}_1 = \frac{\langle G \rangle_1}{\rho_{1^-}} - \frac{\Gamma_{i1}}{c_{1^+} + \rho_{1^-}} \quad (19)$$

and

$$\Gamma_{i1} = \left( \frac{A_i}{A} \right) \frac{(\dot{q}_{li}'' + \dot{q}_{vi}'')_1}{\Delta i_{fg}} \quad (20)$$

Equation (19) shows that the interfacial motion is due to the slug velocity itself plus the added effects of evaporation or condensation mass transfer between the vapor cavity and the slug. Similar relations for the feedwater-vapor interface include

$$\dot{Z}_2 = \frac{G_{fw}}{\rho_{fw}} + \frac{\Gamma_{i2}}{c_2 - \rho_2^+} \quad (21)$$

and

$$\Gamma_{i2} = \left( \frac{A_i}{A} \right)_2 \frac{(\dot{q}_{vi}'' + \dot{q}_{li}'')_2}{\Delta i_{fg}} \quad (22)$$

Note that condensation acts to affect the interface velocity in opposite manners on the two interfaces.

## CALCULATED RESULTS

The parametric slug impact model now consists of equations for the slug itself, Equations (5)-(7), the vapor cavity, Equations (13), (15), and (16),

the four interface Equations (19)-(22), and the necessary equations of state. Note that the vapor cavity is not restricted to single phase saturated vapor but accomodates both two-phase and superheated steam possibilities. On the other hand, the two-phase mixture in the vapor cavity is assumed to be in the homogeneous equilibrium state when it does exist.

For the parametric evaluation, the conditions shown in Table 1 were investigated. Effects of heat transfer coefficient, initial pressure, and relative slug lengths were thus determined over a range of conditions.

#### Effect of Heat Transfer Coefficient

The heat transfer coefficients were varied over a range of 20 with a maximum of  $2 \text{ Mw/m}^2\text{-C}$ . Similar results to those of Florschuetz and Chao[5] for collapsing spherical bubbles were obtained as shown in Figures 2 - 4. For a very high heat transfer coefficient, slug motion is mainly inertia dominated and the steam volume collapse is monotonic. As the heat transfer coefficient decreases, thermal limitations come into play as well due to the decreasing condensation driving potential with decreasing pressure. A coupling between over-acceleration and under-condensation results in oscillitory motion due to

CASE NO.	INITIAL WATER SLUG LENGTH	INITIAL VAPOR CAVITY LENGTH	INITIAL PRESSURE (bar)	$h$ $\text{Mw/m}^2\text{-C}$
1	4D	2D	21.7	2.0
2	4D	2D	21.7	1.0
3	4D	2D	21.7	0.5
4	4D	2D	21.7	0.2
5	4D	2D	21.7	0.1
11	4D	2D	4.48	1.0
12	4D	2D	7.93	1.0
13	4D	2D	42.4	1.0
14	4D	2D	70.0	1.0
21	5.5D	0.5D	21.7	1.0
22	5D	1D	21.7	1.0
23	3D	3D	21.7	1.0
24	2D	4D	21.7	1.0

TABLE 1. Conditions chosen for parametric evaluation of the slug impact model. Pipe diameter, 4.3 cm; Feedwater velocity, 0.9125 m/s; Water temperature, 27C.

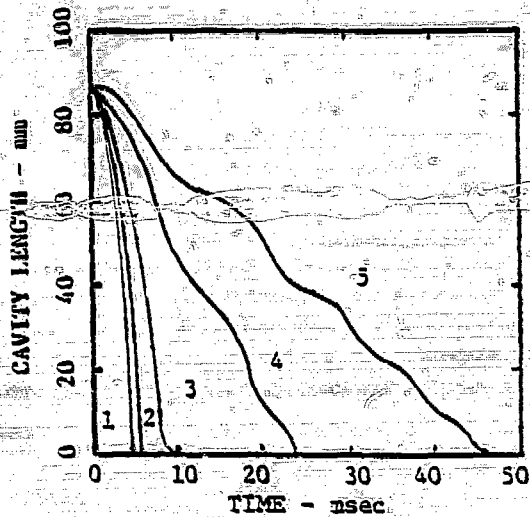


Figure 2. Effect of Heat Transfer Coefficient on Cavity Length. (No. BNL Neg.)

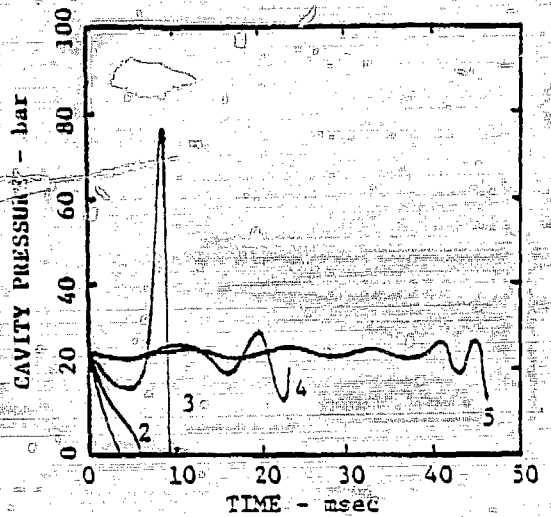


Figure 3. Effect of Heat Transfer Coefficient on Cavity Pressure. (No. BNL Neg.)

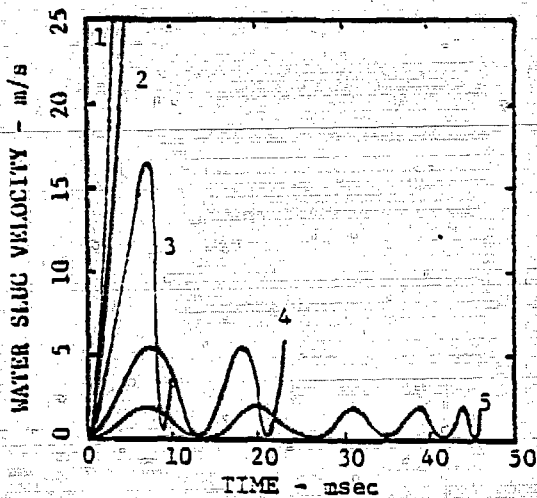


Figure 4. Effect of Heat Transfer Coefficient on Slug Velocity. (No. BNL Neg.)

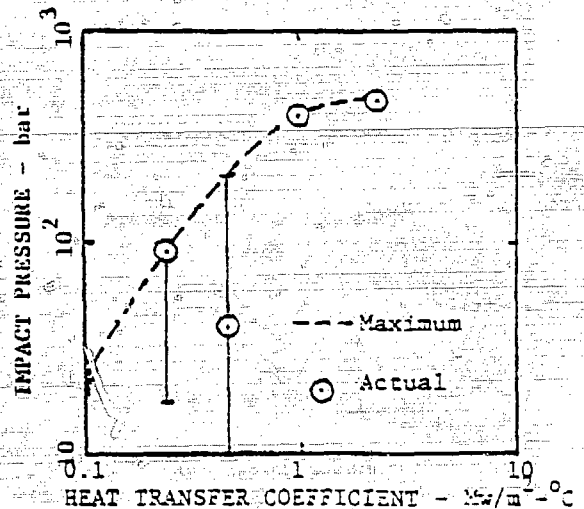


Figure 5. Effect of Heat Transfer Coefficient on Slug Impact Pressure. (No. BNL Neg.)

the cyclic nature of the heat transfer rates which are tied to the saturation temperature according to the cavity pressure. Curve 3 in Figures 2 - 4 indicates that initial depressurization accelerates the slug but also reduces the condensation rate to a value below that required to remove the steam volume displaced by the slug motion. The steam cavity pressure thus rises, decelerating the slug but turning on the condensation again. If there is sufficient time before impact, the process repeats with an ever decreasing period due to the increasing stiffness associated with decreased steam volume.

Impact pressure is calculated as

$$p_i = \rho a v \quad (23)$$

and may vary due to the time in the cycle that impact occurs. While the maximum impact pressure is shown in Figure 5 as the dashed line, (calculated from the slug velocity envelope), the actual value may be quite a bit lower due to the instantaneous velocity at impact. This explains why water hammer in feedwater piping can appear to be a random variable since two sequential slugs are not expected to form in identical fashion.

#### Effect of Slug Initial Pressure

There are expected to be two major effects due to changing the initial pressure. The first effect is the rapidly increased driving potential due to increased saturation temperature in the steam cavity. The second major effect is the increasing vapor density with increased pressure. Thus, at a fixed condensation rate, less percentage of vapor mass per unit time is removed from the cavity resulting in a slower pressure decay rate in the steam cavity. A third but less important effect is the decreasing latent heat tending to offset the second factor. At lower pressures, the effect of increased driving potential dominates, (Figures 6 - 7), while at higher pressures the increase of  $T_s$  with pressure is reduced and the increased vapor density effect dominates.

These effects are seen in the impact pressure, (Figure 8), which first increases then decreases. Again, the apparent randomness due to the oscillatory nature of the collapse is noted.

#### Effect of Relative initial Vapor Cavity Length

The effects of relative cavity length are simply ones of liquid slug inertia balancing against the fraction of vapor mass condensed per unit time. A small cavity and large slug has much liquid inertia and little relative vapor mass. Thus, the pressure falls rapidly causing the slug to accelerate rapidly and impact after a short time, (Figures 9 - 10). As the cavity length increases the pressure decreases more slowly and the acceleration decreases. With sufficiently long cavity size relative to the slug length, however, even though the initial acceleration is slower, over acceleration occurs causing an increase in pressure and deceleration. This is reflected in the decrease with maximum velocity, (Figure 11).

#### Effect of Geometric Scale

Nondimensionalization of the pressure equation for the cavity, Equation (15), shows that the time scale must change linearly in proportion to the length scale to maintain constancy of performance between one geometry and another. Figure 12 shows the results of size on the cavity pressure between a 1/8-scale geometry and a full scale feedwater line. (Note that all other calculations reported herein are for 1/8-scale geometry.) The computed results

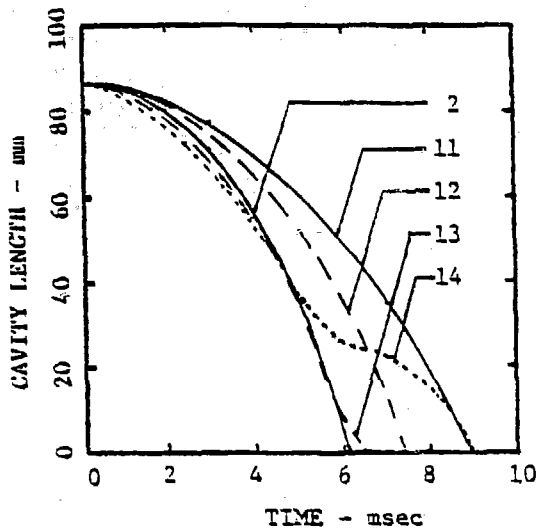


Figure 6. Effect of Initial Pressure on Cavity Length. (No BNL Neg.)

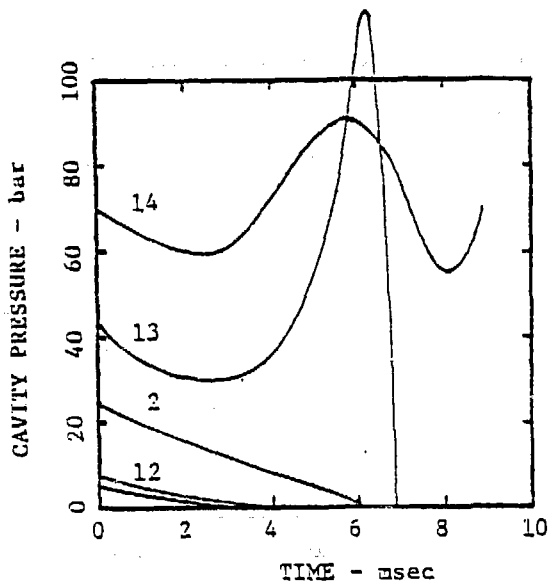


Figure 7. Effect of Initial Pressure on Cavity Pressure. (No BNL Neg.)

confirm the expectation of linear time scaling which, of course, would have to be verified experimentally.

#### INTERNAL VOID COLLAPSE CONSIDERATIONS

Relatively little has been undertaken regarding a vapor cavity collapse in the main feedwater distribution box or inside the tube bundles in an economizer design. The previous analysis indicates that the impact pressure inside a pipe for slug impact depends on the initial relative sizes of the moving liquid mass and vapor cavity involved. Similar considerations may be employed for a model comprised of a spherical shell of liquid of finite mass surrounding a spherical void. While this analysis has not yet been undertaken, it is expected that with increasing relative vapor cavity size, impact pressure will rise up to a point and then become apparently random due to the randomness expected in the formation of the initial geometry. The potential for damage

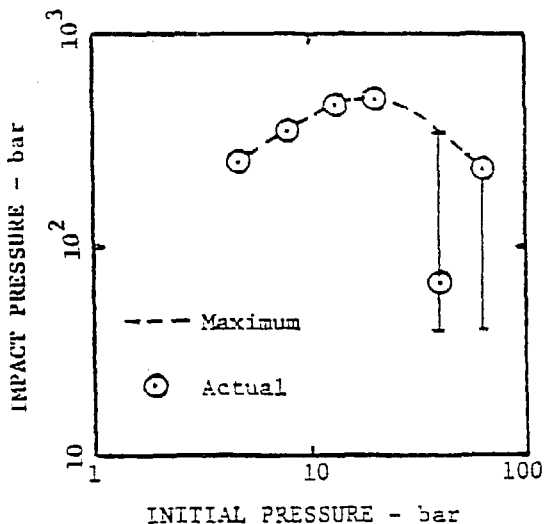


Figure 8. Effect of Initial Pressure on Slug Impact Pressure. (No BNL Neg.)

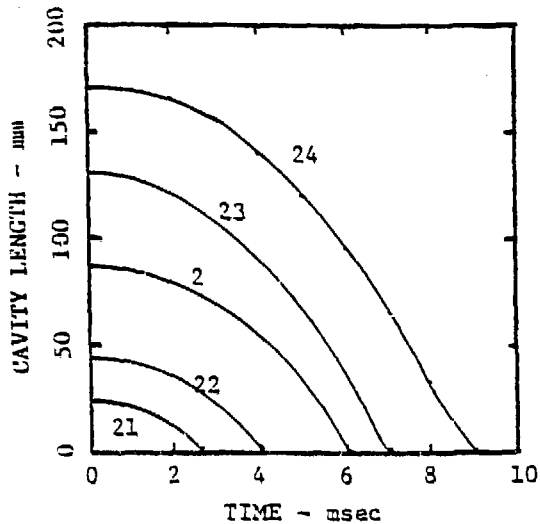


Figure 9. Effect of Initial Relative Cavity Length on Instantaneous Cavity Size. (No BNL Neg.)

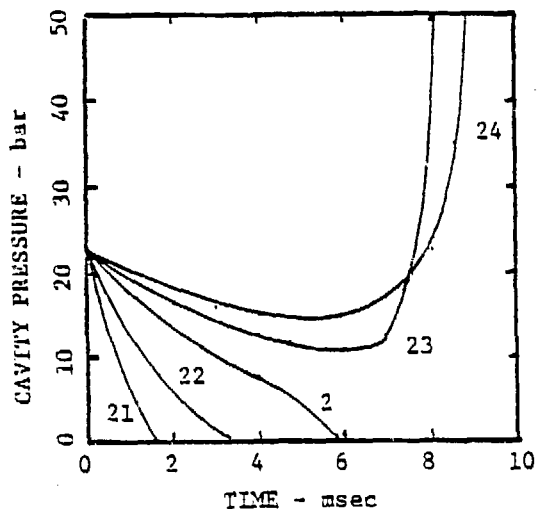


Figure 10. Effect of Initial Relative Cavity Length on Cavity Pressure. (No BNL Neg.)

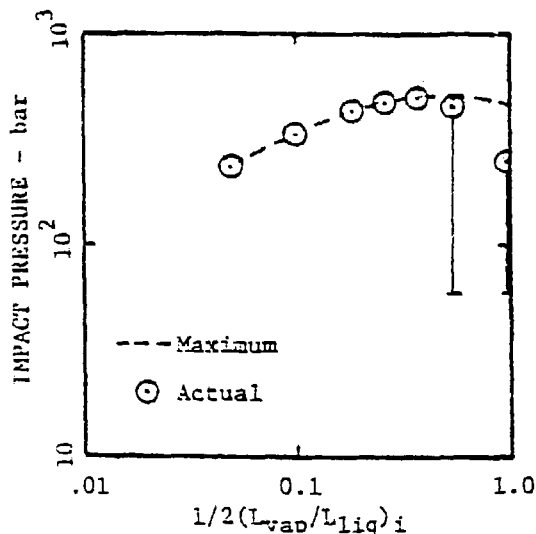


Figure 11. Effect of Initial Relative Cavity Length on Impact Pressure. (no BNL Neg.)

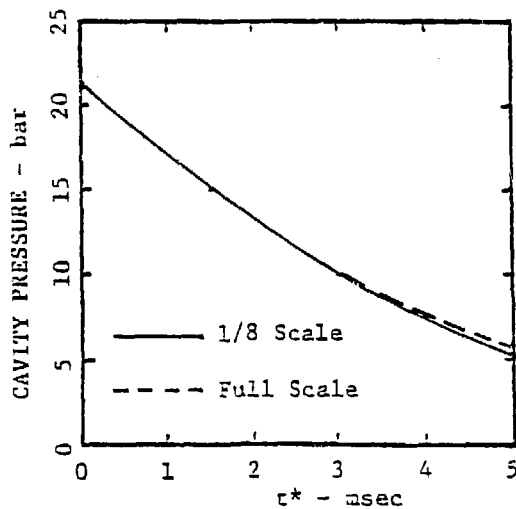


Figure 12. Effect of Geometric Scale. Solid Line - 1/8-Scale,  $t^*=t$ . Dashed Line - Full Scale,  $t^*=t/8$ .  $p_0=20$  bar. (No BNL Neg.)

might then be expected to depend on the ability of pressure pulses to propagate through two phase mixtures. This is the subject of the next section.

### PRESSURE PULSE ATTENUATION

In order to obtain an order-of-magnitude estimate regarding the potential for significant attenuation of the strength of shock waves in two-phase mixtures, a two-phase shock tube experiment was devised and undertaken for both bubbly and slug flow conditions. It is the purpose of this section to describe the experimental apparatus and the results obtained.

#### Experimental Apparatus

The apparatus consisted of two major parts: a shock generator; a test section. As shown in Figure 13, the shock generator consisted of a length of 2.5-cm stainless steel pipe with a rupturable diaphragm at the bottom end, and an ability to measure the internal pressure. The test section consisted of a length of Lexan plastic pipe having a porous plate at the bottom through which air could be injected into the liquid column above. A funnel-shaped device was mounted at the top of the test section to focus the shocks into the test section. Fast response piezoelectric pressure transducers were located at 3.81, 13.97, 26.67, and 39.37 cm from the top of the test section. The porous plate was located in a union, approximately 14 cm below the lowest transducer, 53 cm from the top.

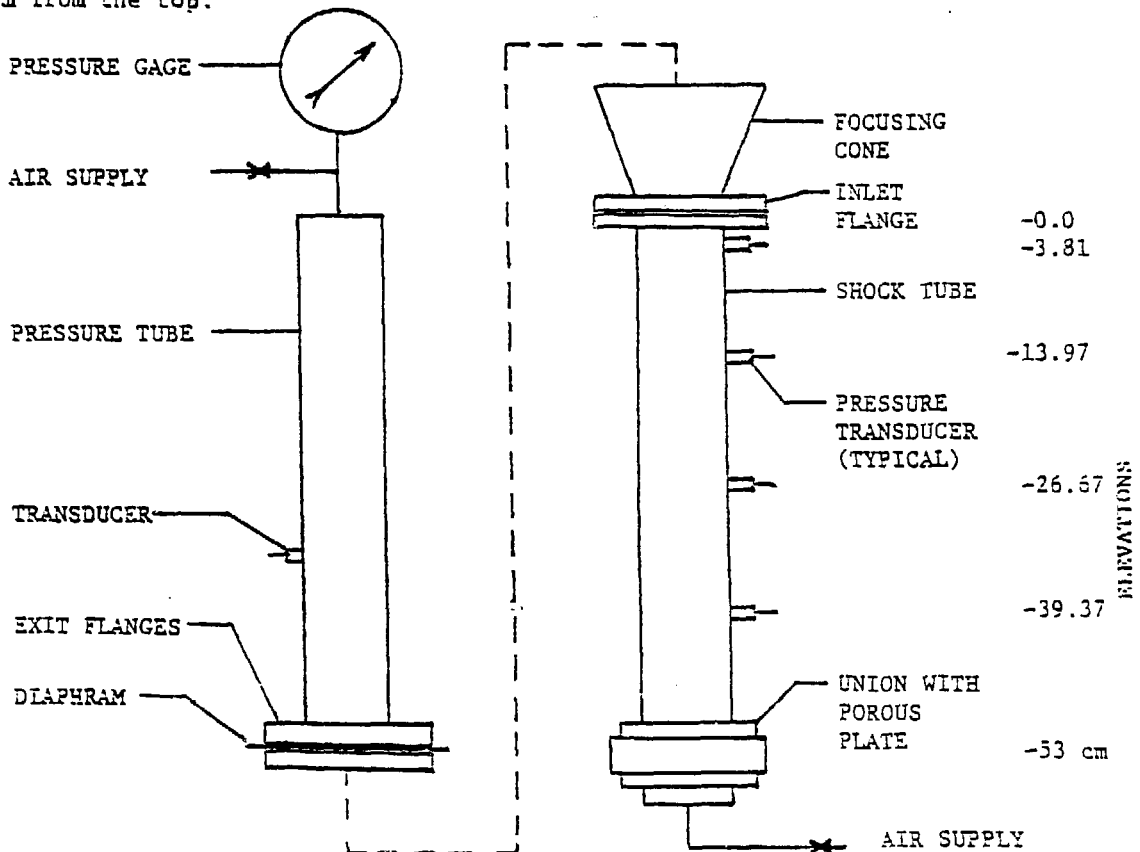


Figure 13. Schematic Diagram of the Shock Tube Experimental Rig. (No BNL Neg.)



The pressure transducers were calibrated by pressurizing the test section with air and then breaking a diaphragm at the top of the test section placed there for that purpose. The response of the pressure transducers was monitored by means of an oscilloscope. The calibration was accurate within approximately  $\pm 10\%$  since these borrowed transducers were designed for 70-bar use, but were being used only at 1-3 bar.

### Experimental Results

Shock tube results for the case of all air are shown in Figure 14 and for all water in Figure 15. The sound speed judged from Figure 14 is approximately 340 m/s compared with an expected value of 347 m/s. Similarly, from Figure 15, the sound speed is approximately 450 m/s which appears reasonably correct for the compliant system of water and plastic pipe. The amplitude of the three pressure signals indicates no visible attenuation in single-phase air or water.

For the case of two-phase bubbly flow at an approximate void fraction of 16%, there appears to be negligible attenuation within the accuracy of the experiment, (Figure 16). The sound speed obtained is about 38 m/s. Similarly, little attenuation is seen in the slug flow case, (Figure 17), at a void fraction of about 33%. In this latter case the sound speed is seen to be variable due to the stochastic nature of the flow structure. This characteristic is shown by the different slopes at similar relative times in the shock passage.

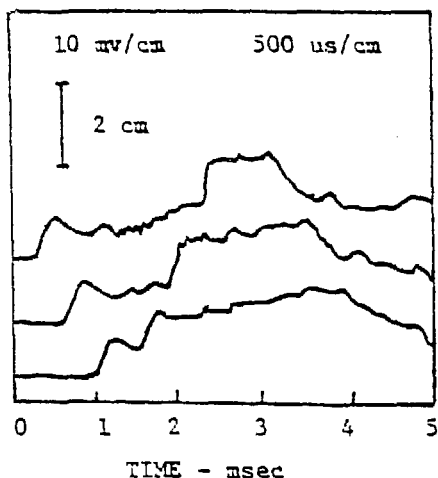


Figure 14. Shock Tube Results for Transducers 12, 13, and 14, for 100% Air. (No BNL Neg.)

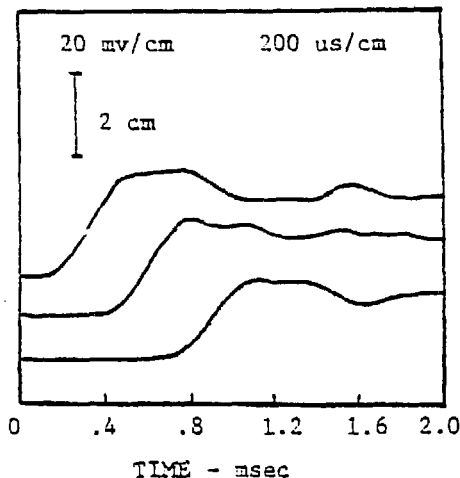


Figure 15. Shock Tube Results for Transducers 12, 13, and 14, for 100% Water. (No BNL Neg.)

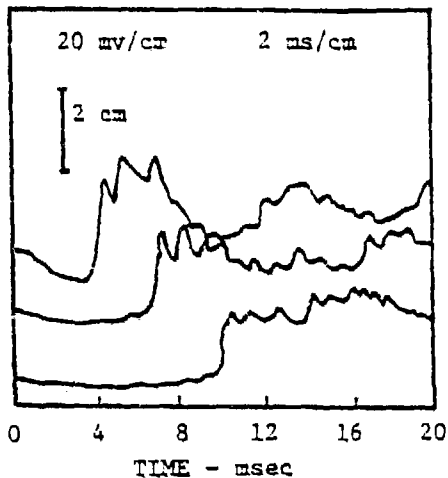


Figure 16. Shock Tube Results Typical of Two-Phase Bubbly Flow. (No BNL Neg.)

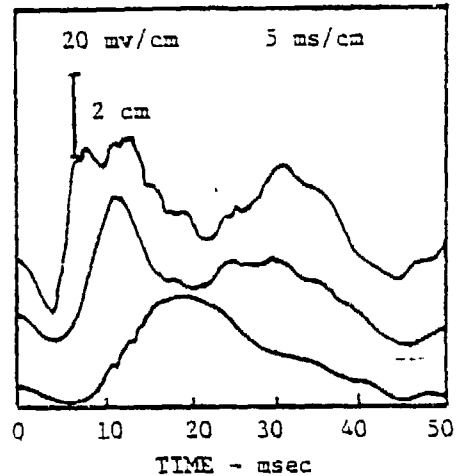


Figure 17. Shock Tube Results Typical of Two-Phase Slug Flow. (No BNL Neg.)

#### CONCLUSIONS AND RECOMMENDATIONS

1. A slug impact model has been developed which has been used for parametric evaluation of water hammer in feeding-type steam generators.
2. The slug impact model shows that similar to bubble condensation analyses and observed behavior, the slug motion may be momentum or thermal dominated, or may oscillate between the two limits due to the interaction between slug motion, vapor cavity pressure, and resultant vapor cavity temperature.
3. Due to the facts summarized in the previous conclusion, there are operating conditions which can lead to oscillatory cavity pressures and slug velocities. This is a possible explanation for the apparent random nature of water hammer observed in experiments. Maximum values may be obtained from this analysis by using the velocity envelope.
4. Interfacial heat transfer coefficient is a major parameter for vapor cavity collapse. The higher the heat transfer, the higher is the expected impact pressure due to cavity collapse.
5. A higher initial pressure causes higher collapse rate at the beginning. However, there seems to be an intermediate pressure which may maximize the impact pressure.
6. Initial cavity size is also important in determining the maximum impact pressure.
7. Similar analysis should be undertaken for localized internal collapse. A simple but seemingly relevant model is one of a spherical shell of liquid of

finite mass surrounding a spherical vapor cavity.

8. The key missing items in the slug impact model are criteria for determining the formation of a slug, its location in the pipe, and its size. Additional criteria needed include the actual heat transfer rates, (probably conduction controlled), effective transfer area, and a coherency factor which would account for less than ideal shocks occurring on impact.

9. Localized void collapse in the inlet downcomer region or internals of an economizer design may behave quite similarly to the slug impact model where initial void size and surrounding liquid mass are expected to be the governing criteria. A key question then arises regarding the degree of attenuation of the resultant shocks due to passage through the two-phase mixture and structure.

10. A simple experiment was performed indicating negligible shock attenuation in bubbly and slug flows for void fractions up to slightly over 30%, within the expected 10% accuracy of the pressure transducers. Thus, the existence of a two-phase mixture does not appear to be a mitigating factor in potential internal water hammer damage.

11. The effects of internal structure on shock dispersion and attenuation should be determined to see if a localized water hammer-induced shock could lead to any damage and the expected extent of such damage.

#### ACKNOWLEDGEMENTS

The authors are indebted to the Westinghouse Electric Corporation for their loan of the pressure transducers used in this series of experiments, and for their assistance in the measurement setup. This work was supported by the U.S. Nuclear Regulatory Commission.

#### REFERENCES

1. W.J. Cahill, "Feedwater Line Incident Report - Indian Point Unit No. 2," Consolidated Edison Cop., AEC Docket No. 50-247, Jan. 14, 1974.
2. J.A. Block, et al., "An Evaluation of PWR Steam Generator Water Hammer," Creare Report, NUREG-0291, June, 1977.
3. R.W. Carlson, "High Pressure Water Hammer Test Program for the Split Flow Preheat Steam Generator," Westinghouse non-proprietary version of a Class 4 proprietary report WCAP-9233, January, 1978.
4. P.Saha, T. Ginsberg, and O.C. Jones, Jr., "Condensation Induced Water Hammer in Preheat Steam Generators," presented at a joint NRC-BNL-Westinghouse meeting, July 21, 1978.
5. L.W. Florschuetz and B.T. Chao, "On the Mechanics of Vapor Bubble Collapse," Trans. ASME, J. Heat Trans., 87C, 209-220, 1965.